THE ASTROPHYSICAL JOURNAL, 602:L25–L28, 2004 February 10

THE FIELD CONDITION: A NEW CONSTRAINT ON SPATIAL RESOLUTION IN SIMULATIONS OF THE NONLINEAR DEVELOPMENT OF THERMAL INSTABILITY

HIROSHI KOYAMA[1,2] AND SHU-ICHIRO INUTSUKA[3]
Received 2003 February 6; accepted 2004 January 2; published 2004 January 30

ABSTRACT

We present the dynamics of a thermally bistable medium using one-dimensional numerical calculations, including cooling, heating, thermal conduction, and physical viscosity. We set up a two-phase medium from a thermally unstable one-phase medium and follow its long-term evolution. To clarify the role of thermal conduction, we compare the results of the two models, with and without thermal conduction. The calculations show that the thermal conduction helps to generate the kinetic energy of translational motions of the clouds. Next, we focus on spatial resolution because we have to resolve the Field length λ_F, which is the characteristic length scale of the thermal conduction. The results show convergence only when thermal conduction is included and a large enough cell number is used. We find it necessary to maintain a cell size of less than $\lambda_F/3$ to achieve a converged motion in the two-phase medium. We refer to the constraint that $\lambda_F/3$ be resolved as the "Field condition." The inclusion of thermal conduction to satisfy the Field condition is crucial to numerical studies of thermal instability (TI) and may be important for studies of the turbulent interstellar two-phase medium: the calculations of TI without thermal conduction may be susceptible to contamination by artificial phenomena that do not converge with increasing resolutions.

Subject headings: hydrodynamics — instabilities — ISM: clouds — methods: numerical

1. INTRODUCTION

The physical properties of turbulence in an interstellar medium (ISM) are considered to be important to the theory of star formation (Nakano 1998; Mac Low & Klessen 2004) and the Galactic ISM (Elmegreen 1999). Arons & Max (1975) proposed that molecular cloud turbulence may be primarily in Alfvenic motions, because for linear-amplitude waves, no compressions are involved. However, the results of numerical magnetohydrodynamic simulations showed that the dissipation time of turbulence is of the order of the flow-crossing time or less (Stone, Ostriker, & Gammie 1998). On the other hand, the triggering of thermal instability (TI) in ISM by strong compressions, and the subsequent production of small-scale structures, has also been studied (Parravano 1987; Hennebelle & Pérault 1999, 2000; Koyama & Inutsuka 2000, hereafter KI00). Recently, Koyama & Inutsuka (2002, hereafter KI02) proposed a mechanism based on TI to generate and maintain tiny clouds with supersonic velocity dispersion in a shock-compressed layer of ISM by performing numerical calculations with radiative heating, cooling, and thermal conduction. Kritsuk & Norman (2002) studied TI-induced turbulence in ISM numerically and measured the monotonic decay of turbulence. In contrast, Vázquez-Semadeni, Gazol, & Scalo (2000) have done large-scale numerical simulations of TI, with and without prescribed energy injection (forcing), and conclude that TI is of minor importance to the resulting spatial and probability distributions of the density field if the interstellar turbulence is driven by stellar and other energetic sources.

Thermal conduction can stabilize TI when the perturbation wavelength is smaller than the Field length $\lambda_F = (KT/\rho^2\Lambda)^{1/2}$ (Field 1965; see description following eq. [4]). If the thermal conduction is not included in the numerical analysis, the perturbations of smaller wavelengths (down to the size of a cell) become unstable so that, in principle, the result depends on the size of the cell in a numerical model. The Field length also determines the width of the intermediate region between the cold medium and surrounding warm medium, in which heating and cooling by thermal conduction balance the radiative heating and cooling (Begelman & McKee 1990). This intermediate region is lost in calculations without thermal conduction. Thus, the inclusion of thermal conduction is necessary to describe the physical evolution of TI and to resolve the critical length scale of TI.

Similar circumstances can be found in hydrodynamical evolution with self-gravity, where the Jeans length plays a critical role. Truelove et al. (1997, 1998) studied the convergence of numerical solutions in isothermal gravitational collapse problems and found it necessary to keep the ratio of cell size to a Jeans length ($\Delta x/\lambda_J$) below 0.25 to avoid artificial fragmentation. They termed this constraint on Jeans instability the "Jeans condition." Bate & Burkert (1997) found a similar criterion for particle methods.

In this Letter, we investigate the convergence property of numerical solutions in TI-induced two-phase gas dynamics. We show how thermal conduction plays a role in the nonlinear development of the TI, and find a necessary condition for the numerical analysis of the nonlinear development of the TI.

2. SIMULATIONS

We solve the following hydrodynamic equations:

$$\frac{\partial \rho}{\partial t} + \frac{\partial}{\partial x}(\rho v) = 0, \tag{1}$$

$$\frac{\partial}{\partial t}\rho v + \frac{\partial}{\partial x}\left(P + \rho v^2 - \frac{4\mu}{3}\frac{\partial v}{\partial x}\right) = 0, \tag{2}$$

[1] Astronomical Data Analysis Center, National Astronomical Observatory, Mitaka, Tokyo 181-8588, Japan.
[2] Current address: Department of Earth and Planetary Sciences, Kobe University, Kobe 657-8501, Japan; hkoyama@kobe-u.ac.jp.
[3] Department of Physics, Kyoto University, Kyoto 606-8502, Japan; inutsuka@tap.scphys.kyoto-u.ac.jp.

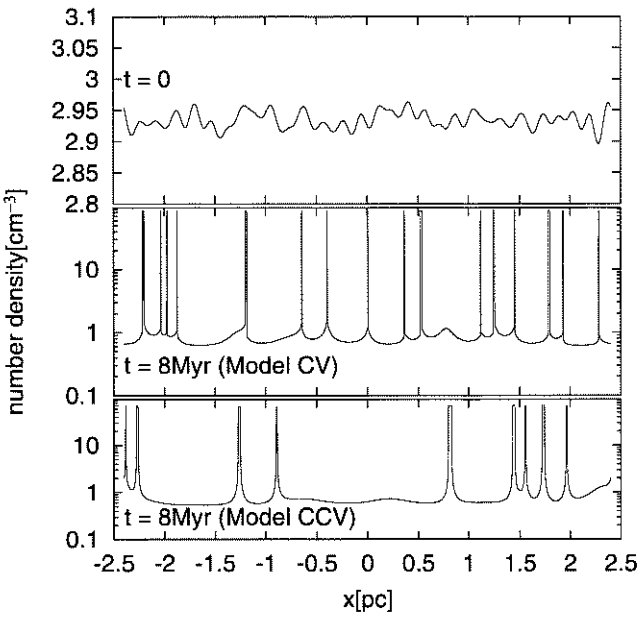

FIG. 1.—Evolution of number density. The number of cells is 16,384. *Top:* initial density profile. *Middle:* Final snapshot for the run without thermal conduction (model CV). *Bottom:* Final snapshot for the run with thermal conduction (model CCV).

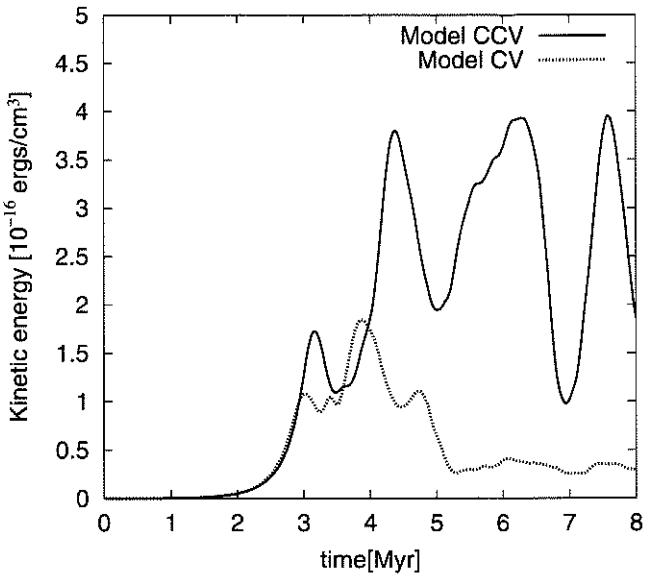

FIG. 2.—Time evolution of the kinetic energy in models CV (*dotted line*) and CCV (*solid line*). The number of cells is 16,384.

$$P = \frac{\rho k_{\rm B} T}{m}, \tag{3}$$

$$\frac{\partial E}{\partial t} + \frac{\partial}{\partial x}\left[(E+P)v - \frac{4\mu}{3} v \frac{\partial v}{\partial x} - K\frac{\partial T}{\partial x}\right] = \frac{\rho}{m}\Gamma - \left(\frac{\rho}{m}\right)^2 \Lambda(T). \tag{4}$$

In the above equations, ρ is the mass density of the gas, v is the velocity of the fluid elements, P is the gas pressure, m is the average particle mass, $k_{\rm B}$ is the Boltzmann constant, $E = P/(\gamma - 1) + \rho v^2/2$ is the total energy per volume, and K is the coefficient of thermal conductivity. For the range of temperatures considered, the dominant contribution to thermal conductivity is that of neutral atoms, for which $K = 2.5 \times 10^3 T^{1/2}$ cm^{-1} K^{-1} s^{-1} (Parker 1953). We assume that the gas consists of monoatomic molecules, and the ratio of the specific heats is $\gamma = 5/3$. The relation between kinetic viscosity μ and thermal conductivity K is characterized by a Prandtl number:

$$\Pr = \frac{\gamma}{\gamma - 1}\frac{k_{\rm B}}{m}\frac{\mu}{K}. \tag{5}$$

In this Letter, we assume the Prandtl number $\Pr = \frac{2}{3}$ for monoatomic molecules. For the heating/cooling function, we adopt a simple fitting formula (see eqs. [4] and [5] in KI02) based on detailed thermal and chemical calculations (KI00).

The adopted hydrodynamical method is the one-dimensional Eulerian code based on the second-order Godunov scheme (van Leer 1979). We use explicit time integration for cooling and heating. We also use explicit time integration for thermal conduction, and physical viscosity with spatially second-order accuracy.

2.1. *Results*

Figure 1 shows the typical numerical results. The length of the computational domain is $L = 4.8$ pc. The boundary conditions are periodic. In this case, cell number of 16,384 is used. Upper panel shows the initial density. The initial condition is a static unstable equilibrium ($\rho/m = 2.93$ cm^{-3}, $T = 756$ K) with a superposition of isobaric density perturbations with wavelengths in the range 0.15 pc $\le |\lambda| \le 4.8$ pc. Here, we introduce the characteristic length scale of TI, λ_a, defined as the sound speed times the cooling time. We can say that perturbations with $\lambda \ge \lambda_a$ correspond to the long-wavelength mode; those with $\lambda_{\rm F} \le \lambda \le \lambda_a$, to the intermediate-wavelength mode. It has been established that the intermediate-wavelength perturbations evolve almost quasistationarily, maintaining quasi-isobaricity throughout their evolution. On the other hand, the long-wavelength perturbations cool before they can equate pressures and therefore develop larger pressure gradients, which then cause them to evolve highly dynamically (Meerson 1996; Burkert & Lin 2000; Sánchez-Salcedo et al. 2002). The λ_a is 0.5 pc in the initial parameters, and thus our simulations include both modes. The middle panel in Figure 1 shows the result of cooling+viscosity models (hereafter model CV). In this case, 17 clouds are formed because smaller wavelength perturbations have larger growth rates of TI. The lower panel in Figure 1 shows the result of cooling+conduction+viscosity models (hereafter model CCV). In this case, however, only nine clouds are shown. Note that all perturbations grow at the initial stage because their wavelengths are larger than the Field length $\lambda_{\rm F} = 0.008$ pc in the initial parameters. The decrease in the cloud number is the consequence of coalescence. Across the interface between the two-phase medium, the conductive heat flux changes the local pressure distribution, and the induced pressure gradient produces gas motion. Thus, the coalescence is driven by thermal conduction.

Figure 2 shows the time evolution of kinetic energy per volume. In the early phase ($0 \le t \le 3$ Myr), the linear perturbation grows. The smaller wavelength perturbations have larger

TABLE 1
RESULTS FROM VARIOUS RESOLUTIONS AT $t = 8$ Myr

		Model CV		Model CCV	
Number of Cells	$\Delta x/\lambda_{F,min}$	Number of Clouds	M^a	Number of Clouds	M^a
32768	0.0488	16	0.054	9	0.134
16384	0.0976	16	0.075	9	0.134
8192	0.1953	17	0.117	9	0.136
4096	0.3906	14	0.138	9	0.167
2048	0.7813	11	0.168	8	0.188
1024	1.5625	8	0.269	8	0.198
512	3.125	6	0.212	6	0.234
256	6.25	5	0.097	6	0.176

[a] Maximum local Mach number.

growth rates and hence evolve rapidly and attain a quasiequilibrium state in short timescales. In the late phase ($t \geq 5$ Myr), the kinetic energy in model CCV (*solid line*) is 1 order of magnitude larger than the case in model CV (*dotted line*). This shows that the kinetic energy of the translational motions are enhanced by the effect of thermal conduction. This shows how thermal conduction plays a role in the nonlinear development of TI.

The conductive-length scale is characterized by the Field length. The Field length is a function of temperature and density, and hence should be defined locally: it varies spatially with a range of 0.6–0.003 pc in this problem. We measured the number of clouds and the maximum local Mach number with various resolutions (Table 1). In model CCV, both numbers converge when the cell size, Δx, is smaller than $0.39\lambda_{F,min}$. In model CV, on the other hand, the results with higher resolutions have larger numbers of clouds and smaller Mach numbers. These resolution-dependent results indicate that the model CVs have a numerical problem. In the absence of thermal conduction, a spatially smooth transition from a cold to a warm phase is impossible, and the spatial distribution of temperature tends to produce discrete jumps from a cold phase to a warm phase. When the cloud moves, the advection between the Eulerian cells produces cells with intermediate and thermally unstable temperatures. Each of these cells becomes unstable, because the most unstable wavelength becomes infinitesimal in the absence of thermal conduction. This thermally unstable cell generates unphysical unstable motion. This artificial noise cannot be removed by increasing the number of cells.

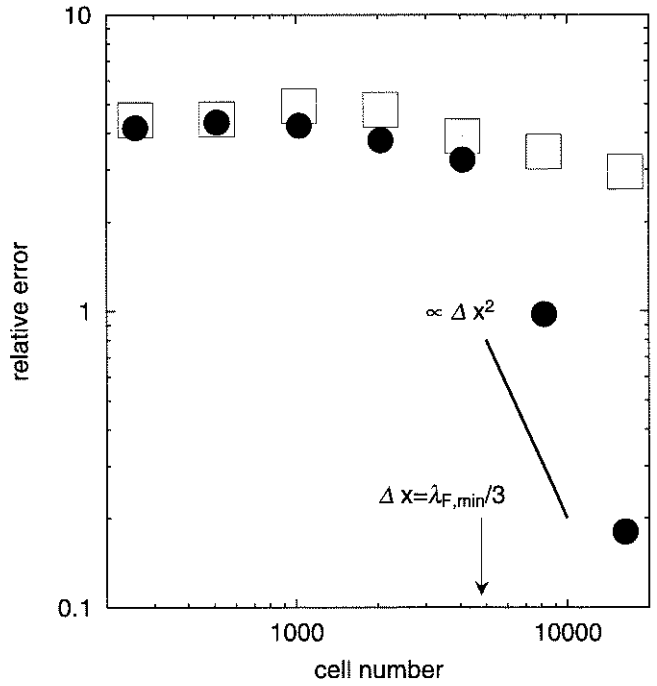

FIG. 3.—Convergence test for density distribution at $t = 8$ Myr. The error function is defined by eq. (6). Model CV (*open squares*) and model CCV (*filled circles*) are presented.

The above results suggest that conductive length scale characterized by the local Field length should be resolved in physically acceptable numerical solutions. Figure 3 shows the convergence test for density distribution at $t = 8$ Myr. The error function is defined as

$$\epsilon_N = \sum_i^N \Delta x_N |\rho_N(x_i, t) - \rho(x_i, t)|, \quad (6)$$

where N is the number of cells and i is the label of cells. We use the result with 32,768 cells as a reference solution: $\rho(x, t) = \rho_{32,768}(x, t)$. The filled circles denote model CCV, and the open boxes denote model CV. Because the numerical scheme we use is spatially a second-order scheme, the numerical errors should decrease with the square of cell length. In the calculations with 256, 512, and 1024 cells, the errors in models CV and CCV are comparable, because neither model resolves Field length. The errors with 4096, 8192, and 16,384 cells in model CCV show second-order convergence, while the amount of error in model CV does not decrease toward second-order accurate solutions. The calculation with 4096 cells uses a uniform cell length, $\Delta x_{4096} = 0.39\lambda_{F,min}$. Therefore, we conclude that we should always use no less than three cells per local Field length to obtain a physically acceptable solution in the calculation of TI. We term this new constraint the "Field condition." The inclusion of thermal conduction is a necessary but not sufficient condition to satisfy the Field condition.

3. DISCUSSION

The thickness of the interface characterized by the Field length is typically much smaller than the physical sizes of the interstellar clouds. Thus, the effect of the thermal conductivity is assumed to be negligible in many numerical studies, with the exception of our own. Our simulations that satisfy the Field condition show more dynamical motions. Let us consider the physical meaning of the difference. For convenience of explanation, we assume the steady state of the two-phase medium.

By integrating hydrodynamic equations over the interface, we obtain

$$(\rho v)^{\rm cold}_{\rm warm} = 0, \quad (7)$$

$$(P + \rho v^2)^{\rm cold}_{\rm warm} = 0, \quad (8)$$

$$[(E + P)v]^{\rm cold}_{\rm warm} = q, \quad (9)$$

where

$$q = \int_{\rm warm}^{\rm cold} \left\{ \left[\frac{\rho(x)}{m}\right]\Gamma - \left[\frac{\rho(x)}{m}\right]^2 \Lambda[T(x)] \right\} dx. \quad (10)$$

Note that the gradients of velocity and temperature are negligible in the region far from the interface, and therefore the net viscosity and thermal conductivity vanish in this integral form. If the integral q vanishes, the set of the equations is equivalent to the Rankine-Hugoniot jump condition. This condition enables us to estimate the difference between preshock and postshock states without solving the detailed structure. In the case of two-phase medium, on the other hand, q does not always vanish: q vanishes only when the pressure is equal to the saturated pressure (Zel'dovich & Pikel'ner 1969). When the thermal conductivity is not included, the corresponding two-phase interface becomes zero thickness, and q vanishes. This is the most essential physical difference between systems with and without thermal conduction. Here we emphasize that the finite value of the integral q should not be ignored—in spite of the small thickness of the interface—because this q causes the time dependence in pressure and hence maintains dynamical motion. It seems impossible to estimate this integral q without knowing the specific structure between the interface. At present, only one method is available for handling this problem—the use of a high spatial resolution to describe the detailed interface structure. The need for the spatial resolution of the Field length does not require the spatial resolution of shock fronts because the former is much larger than the latter:

$$\lambda_{\rm F} = \sqrt{\frac{KT}{\rho^2 \Lambda}} \sim l\sqrt{\frac{t_c}{t_{\rm mfp}}} > l, \quad (11)$$

where l is the mean free path, and t_c and $t_{\rm mfp}$ are the cooling time and mean flight time, respectively.

4. CONCLUSION

In this Letter, we investigate the dynamical evolution of TI using one-dimensional hydrodynamical calculation, including heating, cooling, thermal conduction, and physical viscosity. We present the results of the convergence tests, with and without thermal conduction. Our findings are as follows:

1. The simulations without thermal conduction show that the results are resolution dependent. The majority of the clouds are formed in higher resolution runs. The maximum local Mach number decrease with increasing resolution.
2. The translational motions survive in the calculations with thermal conduction and sufficient spatial resolution. This shows that thermal conduction helps to generate the kinetic energy of the translational motions of the two-phase medium. We found the maximum local Mach number to be 0.13 at $t = 8$ Myr in the numerical model.
3. At least three cells are required to resolve the crucial length scale, the Field length, to attain the convergence of the numerical calculations. We refer to this constraint as the "Field condition." The inclusion of thermal conduction is imperative to satisfy the Field condition.

Numerical computations were carried out on VPP5000 at the Astronomical Data Analysis Center of the National Astronomical Observatory, Japan (NAOJ). This work was supported in part by the 21st Century COE Program of Origin and Evolution of Planetary Systems in the Ministry of Education, Sports, Science, and Technology (MEXT). We thank the Astronomical Data Analysis Center of NAOJ for financial support for publication.

REFERENCES

Arons, J., & Max, C. E. 1975, ApJ, 192, L77
Bate, M. R., & Burkert, A. 1997, MNRAS, 288, 1060
Begelman, M. C., & McKee, C. F. 1990, ApJ, 358, 375
Burkert, A., & Lin, D. N. C. 2000, ApJ, 537, 270
Elmegreen, B. G. 1999, ApJ, 527, 266
Field, G. B. 1965, ApJ, 142, 531
Hennebelle, P., & Pérault, M. 1999, A&A, 351, 309
———. 2000, A&A, 359, 1124
Koyama, H., & Inutsuka, S. 2000, ApJ, 532, 980 (KI00)
———. 2002, ApJ, 564, L97 (KI02)
Kritsuk, A. G., & Norman, M. L. 2002, ApJ, 569, L127
Mac Low, M.-M., & Klessen, R. S. 2004, Rev. Mod. Phys., 76, 125
Meerson, B. 1996, Rev. Mod. Phys., 68, 215
Nakano, T. 1998, ApJ, 494, 587
Parker, E. N. 1953, ApJ, 117, 431
Parravano, A. 1987, A&A, 172, 280
Sánchez-Salcedo, J., Vázquez-Semadeni, E., & Gazol, A. 2002, ApJ, 577, 768
Stone, J. M., Ostriker, E. C., & Gammie, C. F. 1998, ApJ, 508, L99
Truelove, J. K., Klein, R. I., McKee, C. F., Holliman, J. H., II, Howell, L. H., & Greenough, J. A. 1997, ApJ, 489, L179
Truelove, J. K., Klein, R. I., McKee, C. F., Holliman, J. H., II, Howell, L. H., Greenough, J. A., & Woods, D. T. 1998, ApJ, 495, 821
van Leer, B. 1979, J. Comput. Phys., 32, 101
Vázquez-Semadeni, E., Gazol, A., & Scalo, J. 2000, ApJ, 540, 271
Zel'dovich, Y., & Pikel'ner, S. 1969, Soviet Phys.–JETP, 29, 170